Classification of supernovae with J-VAR

Juan Antonio Molina Calzada
Summer internship at CEFCA
Supervisor: Alessandro Ederoclite

Abstract

The Javalambre Variability Survey (J-VAR) offers a significant opportunity to deepen our understanding of transient astronomical events, with a particular focus on supernovae (SNe). In this study, we concentrate on the core-collapse supernova SN 2023ixf, conducting an extensive photometric analysis using data from the Tx40 telescope (with three filters) and the JAST80 telescope (utilizing the seven J-VAR filters) at the Observatorio Astrofísico de Javalambre (OAJ). We model the supernova's light curves with a decay model and a sncosmo model, extracting key evolutionary parameters despite challenges such as the absence of early observations before peak brightness and substantial discrepancies in the redder bands. Our results align with the expected features of a Type II-P supernova. Following the characterization of SN 2023ixf, we extend our analysis to the PESSTO (Public ESO Spectroscopic Survey of Transient Objects) catalogue, which provides spectral evolution data for various transients. By applying synthetic photometry to these spectra and using the stretch method, we derive light curve templates for the seven J-VAR filters across different transient types, although significant issues were encountered with the stretch method. The goal is to create a classification algorithm based on these templates. This study positions the J-VAR project to play a crucial role in the classification and analysis of future transient detections.

1 Introduction

The Javalambre Variability Survey (J-VAR) represents a significant advancement in the study of transient astronomical phenomena, with a specific emphasis on supernovae (SNe). Supernovae are among the most energetic events in the universe, marking the explosive deaths of massive stars or the thermonuclear detonations of white dwarfs in binary systems. These cosmic events not only illuminate the final stages of stellar evolution but also play a crucial role in dispersing heavy elements throughout the universe, contributing to the formation of new stars, planets, and even life.

Historically, the study of supernovae has evolved significantly from the early observations of these explosive events to the sophisticated multi-wavelength surveys conducted today. The discovery of supernovae dates back to the 1604 supernova in the constellation Ophiuchus, which was observed by Johannes Kepler. This supernova, known as Kepler's Supernova, was the last supernova observed in our galaxy for over 300 years. The 20th century saw a revolution in our understanding of supernovae, with the development of theoretical models and observational techniques that expanded our knowledge of their origins and types. Key milestones included the development of the standard candle method for Type Ia supernovae, which has been instrumental in measuring cosmic distances and discovering the accelerated expansion of the universe.

The advent of large-scale surveys in the late 20th and early 21st centuries, such as the Sloan Digital Sky Survey (SDSS) and the Pan-STARRS1 survey, further transformed our approach to studying supernovae. These surveys provided vast amounts of data, allowing astronomers to study supernovae in greater detail and with improved statistical significance. The Supernova Legacy Survey (SNLS) and the Dark Energy Survey (DES) continued this trend, offering insights into the diversity of supernovae and their role in cosmology.

In this context, the Javalambre Variability Survey (J-VAR) emerges as a contemporary initiative designed to extend our observational capabilities further. Conducted at the Observatorio Astrofísico de Javalambre (OAJ) in Spain, J-VAR leverages advanced photometric techniques and a wide-field observational approach to capture and analyze transient astronomical events. The survey employs the Tx40 and JAST80 telescopes, equipped with a range of filters, to monitor and analyze these events in unprecedented detail.

In this study, we focus on the core-collapse supernova SN 2023ixf, a recent addition to the diverse catalogue of supernovae observed by J-VAR. SN 2023ixf, located in the spiral galaxy M101, was first detected on May 19, 2023, by an amateur astronomer in Japan. This supernova was subsequently observed by various telescopes, including those at OAJ. Our analysis utilizes photometric data from the Tx40 telescope, which observes in three filters, and the JAST80 telescope, which uses seven filters provided by the J-VAR survey.

To understand the behaviour of SN 2023ixf, we model its light curves using the Bazin function and the sncosmo models. These models allow us to extract crucial evolutionary parameters, despite some challenges such as the lack of early observations before peak brightness and discrepancies in the redder bands of the spectrum. Our results align with the characteristics expected of a Type II-P supernova, characterized by a plateau phase in its light curve following peak brightness.

The J-VAR project is designed to address the challenges of transient astronomy by providing a comprehensive photometric dataset across multiple filters. The J-VAR uses a set of 7 filters to capture detailed light curves, with observations made under various weather conditions. To ensure the accuracy of our data, we correct for magnitude offsets by comparing J-VAR observations with reference data from the J-PLUS survey, which was observed under clear conditions.

In addition to photometric analysis, we extend our study to include spectral data from the Public ESO Spectroscopic Survey of Transient Objects (PESSTO). PESSTO, utilizing the ESO New Technology Telescope, provides detailed spectroscopic coverage of a wide range of transient objects, including supernovae. By applying synthetic photometry to PESSTO's spectral data, we generate light curve templates for different transient types, although we encountered challenges with the stretch method used for template fitting.

Our study highlights the potential of the J-VAR project in advancing the classification and analysis of supernovae and other transients. The combination of photometric and spectroscopic data offers a comprehensive view of these dynamic events, contributing to our understanding of their physical properties and evolutionary stages. As we continue to explore and analyze transient phenomena, the integration of diverse datasets and advanced observational techniques will be crucial in unravelling the complexities of the universe's most explosive events.

2 Objectives

The J-VAR project is dedicated to advancing time-domain astrophysics at the OAJ, with a key focus on studying supernovae. To illustrate our approach, we use SN 2023ixf as a case study (Section 6). This Type IIP supernova has been observed using both the JAST80 telescope and the supplementary Tx40 telescope. Our analysis will involve examining the photometric data of SN 2023ixf and modelling this type of supernova.

In the second phase of the project, we will utilize spectroscopy data from the PESSTO project to create a comprehensive dataset for characterizing various transients using J-VAR's unique filter set (Section 7). The goal is to develop light curve templates for each type of SNe and subsequently create a classification algorithm based on these templates.

3 What is J-VAR?

The Javalambre Variability Survey (J-VAR) is a comprehensive astronomical project designed to explore time-domain astrophysics from the Javalambre Astrophysical Observatory (OAJ). J-VAR is dedicated to studying the variability of celestial objects, leveraging the observatory's T80Cam and JAST/T80 telescope. This survey utilizes a subset of the J-PLUS photometric system, focusing on a selection of seven bands (Figure 1) that span broad and narrow wavelength ranges, including both optical and near-infrared filters.

The chosen bands, specifically the gri broad bands and narrow bands $J0395$, $J0515$, $J0660$, and $J0861$, are strategically selected to maximize observational efficiency and minimize time spent in low-throughput regions (Figure 2).

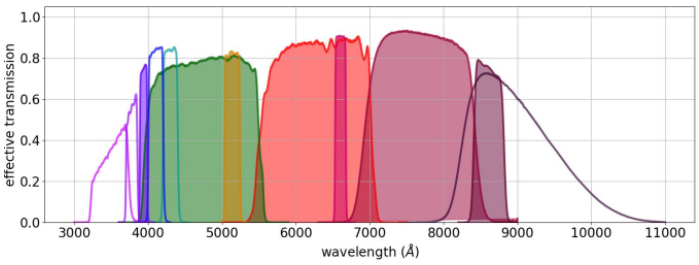

Figure 1: Effective transmission of the 7 different J-VAR filters. From left to right: J0395, g, J0515, r, J0660, I, and J0861

The primary goal of J-VAR is to monitor and analyze

variations in light from astronomical sources, which can reveal crucial information about phenomena such as supernovae, variable stars, and other transient events. By operating in tandem with other major surveys and space missions, J-VAR aims to complement and enhance our understanding of the dynamic universe. The survey's observational strategy includes monitoring selected patches of the sky previously covered by J-PLUS, which allows for detailed variability studies.

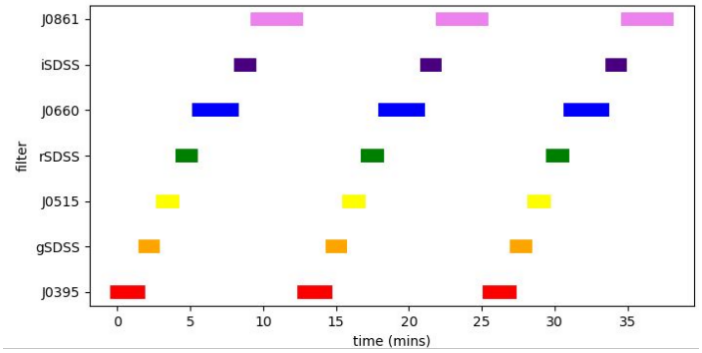

Figure 2: The muli-epoch J-VAR mode employed for the study of the different transits. Each field is visited 11 times taking 3 sets of images using the 7 filters.

Additionally, J-VAR's data are collected during both photometric and non-photometric nights, aiming to extend the depth of observations and increase the likelihood of detecting transient events. This dual approach ensures a robust dataset, crucial for advancing time-domain astrophysics and providing valuable insights into the evolving universe. Figure 3 shows the currently covered sky regions.

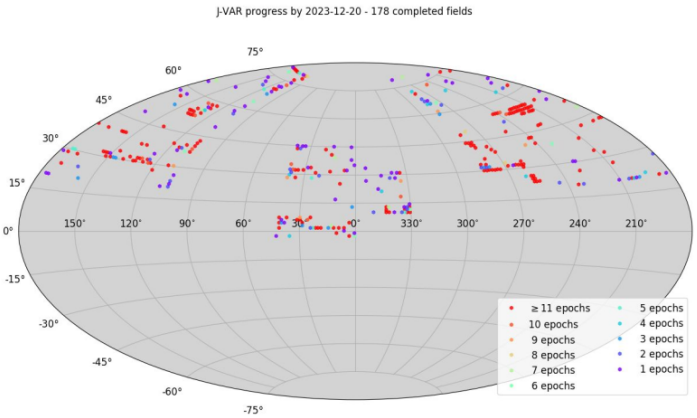

Figure 3: Region sky map showing the J-VAR progress by 2023-12-20. 178 fields have been completed.

4 What is PESSTO?

The Public ESO Spectroscopic Survey of Transient Objects (PESSTO) is a project utilizing the ESO New Technology Telescope equipped with the EFOSC2 (optical) and SoFi (near-infrared) spectrographs. As one of two public spectroscopic surveys currently running at ESO, PESSTO aims to classify and monitor transient astronomical phenomena, such as supernovae and other unusual optical transients. With the advent of wide-field optical telescopes and digital cameras capable of surveying almost the entire sky in less than a month, PESSTO is discovering new classes of transients that challenge our understanding of the physics behind these explosions. This project highlights the diversity in the transient Universe, influenced by factors such as progenitor stellar mass, metallicity, binarity, and rotation. Figure 4 shows the different types of transients as a function of brightness and decay time.

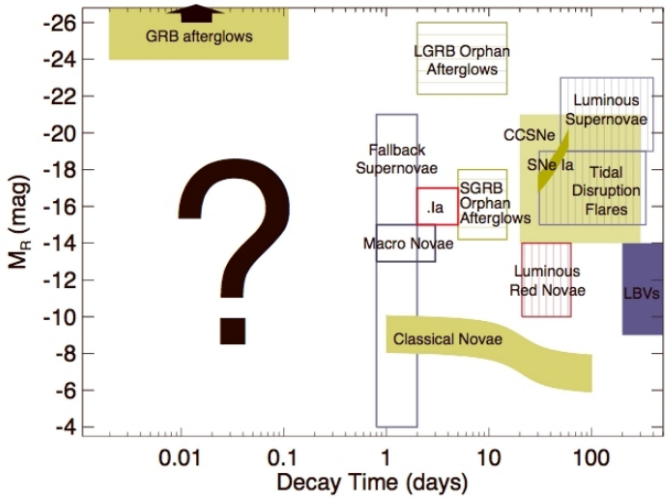

Figure 4: Distribution of the different types of transients in the function of each luminosity and time variably. Figure extracted from Rau et al. (2009).

PESSTO aims to provide comprehensive spectroscopic data for around 2000 supernovae, with detailed time series coverage for approximately 150 of these objects. The project, spanning over four years with a possible extension pending review, partners with surveys like La Silla-Quest, SkyMapper, Pan-STARRS1, and CHASE. All raw data from PESSTO are publicly accessible through the ESO archive, facilitating extensive research and discovery. PESSTO has classified nearly 4000 transients and has analyzed a substantial number of these events, contributing significantly to the field of transient astronomy.

5 Definitions

Chandrasekhar limit

The Chandrasekhar limit defines the maximum mass a stable white dwarf can have before it collapses under its gravity, potentially forming a neutron star or black hole. This limit is approximately 1.4 $M_{\odot}$, though it can vary slightly depending on factors such as metallicity (Z). When a white dwarf exceeds this mass threshold, the electron degeneracy pressure—responsible for counteracting gravity in white dwarfs—becomes insufficient to prevent collapse, leading to a gravitational implosion.

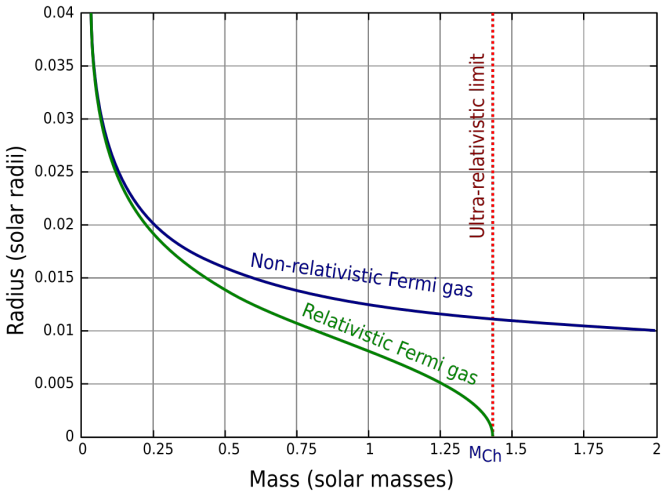

Figure 5: Radius-mass relation for a model white dwarf using general pressure law for an ideal Fermi gas (green) and a non-relativistic ideal Fermi gas (blue). The horizontal line shows the ultra-relativistic limit (Chandrasekhar mass limit).

Alternatively, the Chandrasekhar limit can be conceptualized as the maximum mass at which a white dwarf's radius can shrink to zero due to gravitational forces. This perspective highlights the inverse relationship between a white dwarf's mass and its radius: as the mass increases, the radius contracts until the white dwarf can no longer support itself against collapse.

Supernovae

A supernova is a spectacular and intense explosion during the final stages of a massive star's life. This dramatic event results in the ejection of the star's outer layers into space, producing a brilliant flash of light that can briefly outshine an entire galaxy. Supernovae are vital to the universe as they distribute elements heavier than hydrogen and helium—key ingredients for planet formation and the emergence of life. They often leave behind intriguing remnants, such as neutron stars or black holes.

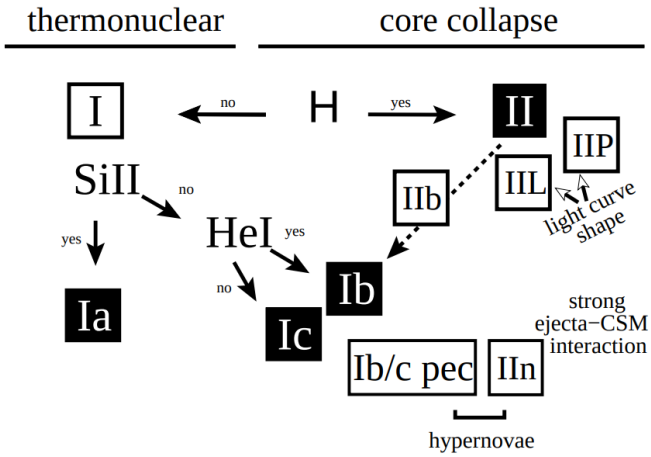

Figure 6: The current classification scheme of supernovae. Type Ia SNe is associated with the thermonuclear explosion of accreting white dwarfs. Other SN types are associated with the core collapse of massive stars. Some Ib/c and IIn SNe with explosion energies E > 1052 erg is often called hypernovae. Figure extracted from Turatto (2003).

Supernovae are categorized based on their light curves and spectral features, particularly the presence or absence of specific absorption lines. They are primarily divided into two types: Type I and Type II. Type I supernovae lack hydrogen lines in their spectra and are further subdivided into Type Ia, which shows singly ionized silicon (Si II) line and results from a thermonuclear explosion in a white dwarf; Type Ib, which features weak or no silicon absorption and non-ionized helium (He I) line, typically arising from core collapse in massive stars that have shed their hydrogen envelopes; and Type Ic, which lacks both helium and hydrogen lines and results from core collapse with extensive layer stripping. Type II supernovae, on the other hand, exhibit hydrogen lines and are classified based on their light curves: Type II-P shows a "plateau" in brightness before declining, Type II-L displays a "linear" decrease in luminosity, Type IIn features narrow lines indicative of interaction with surrounding material, and Type IIb transitions from Type II characteristics to resemble Type Ib as the explosion progresses. Figure 6 shows this classification.

6 SN2023ixf

The first part of this study focuses on the supernova SN2023ixf, which was discovered in the M101 galaxy. This supernova was initially detected on May 19, 2023, by an amateur Japanese astronomer. Following its discovery, several telescopes began observing the event, including the Tx40 and JAST80 telescopes from the OAJ.

The Tx40 telescope is a 40 cm instrument, mounted on a DMM160 mount, and is equipped with an FLI camera featuring a 1k x 1k scientific-grade CCD, providing a 13' x 13' field of view. Although the Tx40 is primarily dedicated to measuring atmospheric extinction each night at the OAJ by monitoring stars across 10 optical filters at varying air masses, it was pointed at the supernova as an exception. The telescope remains fully operational and continues to collect data routinely.

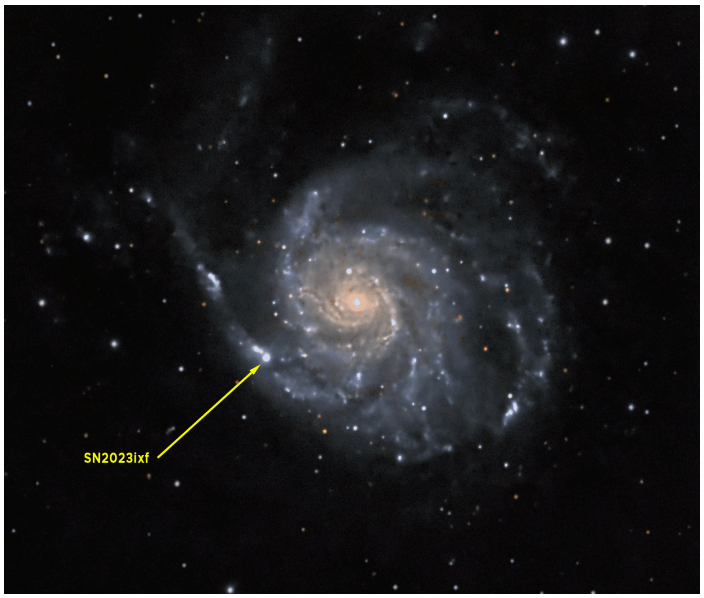

Figure 7: Image of M101 galaxy shortly after the SN explosion. The SN2023ixf is marked with a yellow arrow. Image taken by astrophotographer Patrick A. Cosgrove.

6.1 Light curve with Tx40

Decay model

For the study of SN2023ixf, data were collected using the three SDSS filters of the Tx40 telescope: gsdss, rsdss, and isdss. Observations of the supernova began on May 27, 2023, which was 8 days after its discovery and after the peak of the light curve. This delay presents a challenge, as missing the peak means that some critical information was not captured. Nevertheless, the data collected post-peak were measured with high accuracy and at consistent intervals, from the first to the last data point on the light curve. Magnitude measurements continued for 90 days until the brightness had decreased significantly from the peak. Consequently, the light curves of SN2023ixf were fitted for the three different filters, as shown in Figure 8.

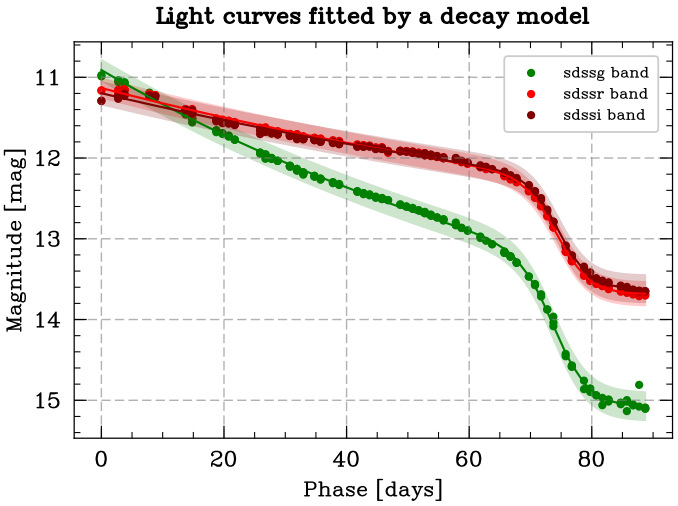

Figure 8: Light curve, using Tx40 data, fitted for the SN2023ixf by using the Bazin function for the sdssg, sdssr, and sdssi bands. The shadows are the associated error of the fits. t = 0 days was set for the first measured.

For the fit of the light curves, we have employed a decay model given by the Bazin function (Bazin et al. 2009) (Equation 1).

$$f(t) = A \cdot \frac{e^{-(t-t_0)/\tau_{fall}}}{1 + e^{-(t-0)/\tau_{rise}}} + B \qquad (1)$$

This function explains the physics of the light curve by using 5 parameters: A, B, τ_{fall}, τ_{rise}, and t_0. The first two, A and B, are a normalization and a constant term, respectively. The τ_{fall} and τ_{rise} parameters measure the declining and rising of the light curve, respectively. Lastly, using the parameter t_0, the peak day can be obtained by using the following relation.

$$t_{max} = t_0 + t_{rise} \cdot Ln(\frac{\tau_{fall}}{\tau_{rise}} - 1) \qquad (2)$$

By using the *lmfit* package of Python, these parameters can be obtained by doing a least-squares fit. Table 1 lists estimated parameters for the different bands.

The obtained parameters are consistent with the selection criteria of Dai et al. (2018), except for τ_{rise}. This pa-

Table 1: Fitted parameters, using the Bazin function, of the light curves of SN2023ixf for the different g-, r-, and isdss bands with their associated error derived from the fit.

	gsdss	rsdss	isdss
A[mag]	-1.887 ± 0.012	-1.438 ± 0.011	-1.388 ± 0.012
B[mag]	15.083 ± 0.011	13.6866 ± 0.0093	13.622 ± 0.011
τ_{fall}[days]	2.787 ± 0.060	2.619 ± 0.067	2.453 ± 0.076
τ_{rise}[days]	-2.873 ± 0.063	-2.673 ± 0.069	-2.500 ± 0.079
t_0[days]	74.100 ± 0.080	74.482 ± 0.084	74.776 ± 0.096

rameter is expected to be greater than 1. This discrepancy can be attributed to the absence of data from the days preceding the peak. Consequently, the negative value for τ_{rise} likely reflects the loss of data points in the peak. The remaining parameters fall within the quality ranges established by Dai et al. (2018). These criteria were designed to standardize the selection process for large datasets of SNe measurements.

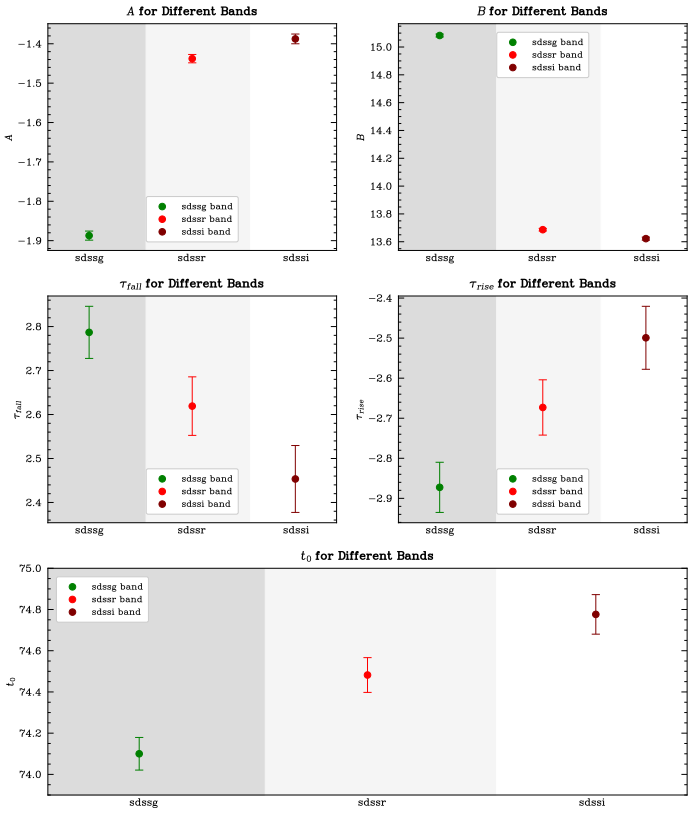

Figure 9: Relations between the fitted parameters (A, B, τ_{fall}, τ_{rise}, and t_0) of SN2023ixf and the g-, r-, and isdss bands, using Tx40 data. Errors are derived from the fit.

Figure 9 illustrates the relationship between the fitted parameters and the bands. This relationship is further explained by the colour variation of SN 2023ixf, which will be detailed later (see Figure 14).

Lastly, another important parameter for classifying supernovae is Δm_{15}, which measures the difference between the apparent magnitude in a given band at the peak and 15 days afterwards. In our observations with the Tx40 telescope, we only have data for the g-, r-, and i-bands. Consequently, the Δm_{15} values reported are estimates based on these bands. Table 2 presents the Δm_{15} values for the g-, r-, and i-bands.

Table 2: Δm_{15} for the g-, r-, and i-bands with their associated error, calculated by first-order error propagation.

	gsdss	rsdss	isdss
Δm_{15}[mag]	0.62 ± 0.18	0.28 ± 0.17	0.26 ± 0.20

sncosmo model

Another approach to fitting the light curve of a supernova is to use a predefined model from the *sncosmo* package[1], a Python library specialized in supernova analysis. *sncosmo* provides tools for modelling the spectral and light curve evolution of supernovae, allowing researchers to fit observational data with either predefined or custom models, handle different photometric filters, and perform analyses such as redshift correction and light curve fitting.

Based on the light curve shown in Figure 8 and the parameters obtained in Table 1, SN2023ixf can be classified as a Type IIP supernova due to its characteristic plateau after the peak and a relatively short τ_{fall}. This classification is supported by some authors, such as Pledger & Shara (2023), despite some discrepancies.

Figure 10 shows the fitted light curve of SN2023ixf using the 'nungent-sn2p' model from *sncosmo* for the three sdss bands. This model provides the best fit to the

[1] https://sncosmo.readthedocs.io/en/stable/index.html

SN2023ixf light curve, as evidenced by the smallest residuals. Other models tailored for different supernova types yielded higher residuals, reinforcing the Type IIP classification. However, there are some issues, particularly in the redder bands. Notably, a few days after the peak, the *sncosmo* model predicts a secondary peak that is not observed in our data. While some supernovae, such as Type IIb, exhibit two peaks, SN2023ixf is a Type IIP and should not have it. This discrepancy highlights an area for further investigation in future work. In addition, the gsdss bands have also problems with the last data points.

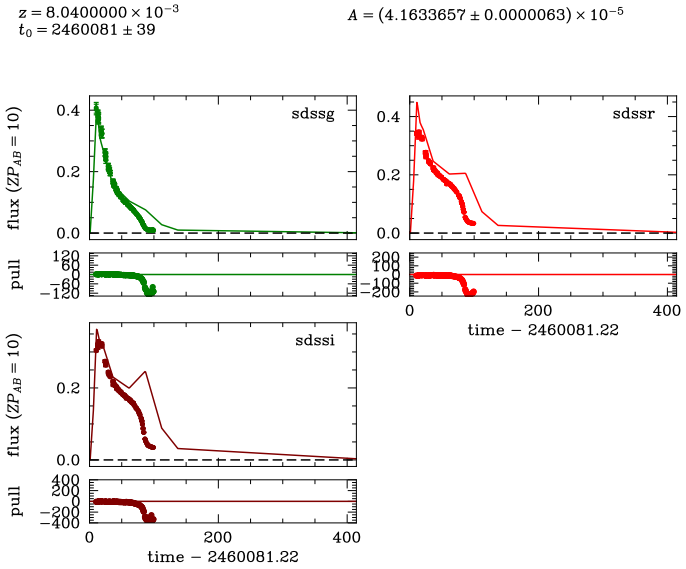

Figure 10: Light curves, using Tx40 data, fitted for the SN2023ixf by using the "nungent-sn2p" model for the sdssg (green), sdssr (red), and sdssi (maroon) bands. Pulls correspond to errors associated with the differences between the observations and the model. The fitted model parameters, A and t_0, are also fitted at the top. The error bars are not noticeable because of their small value.

6.2 Light curve with JAST80

Another key objective of this project is to evaluate whether the J-VAR project, which employs the JAST80 telescope, can effectively detect supernova light curves across all 7 filters while surveying the celestial sphere. To achieve this, we analyzed the J-VAR data collected in the vicinity of M101, where SN2023ixf is located, by performing a cross-match with a precision of 2 arcsec. Additionally, we used data from the J-PLUS project, as well as other OAJ surveys of star-forming galaxies, to correct for magnitude offsets. While J-PLUS observes under clear sky conditions, J-VAR often operates in less favourable weather. This discrepancy can be addressed by calculating and applying these offsets. We selected J-PLUS for calibration instead of other surveys such as SDSS or Pan-STARRS because J-PLUS uses the same instruments as J-VAR, ensuring greater compatibility and accuracy.

Growth curve and offsets

To calculate the magnitude offsets, we performed a cross-match between the J-VAR data (analyzed in this study) and the J-PLUS reference catalogue to determine the differences (offsets) in magnitudes for reference stars. As mentioned, J-VAR operates under non-photometric conditions, while J-PLUS operates under high-quality, clear-sky conditions. Thus, applying these calculated offsets should correct the J-VAR data to align with the more accurate J-PLUS measurements.

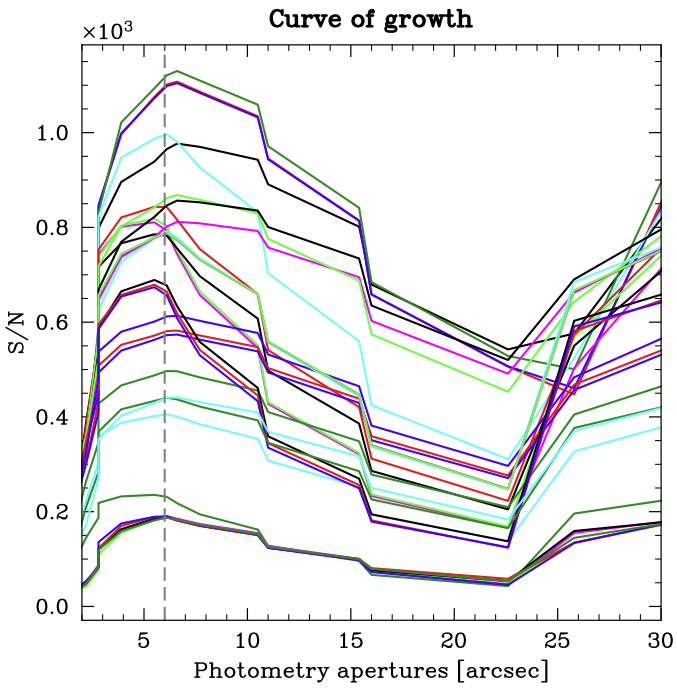

Figure 11: Curve of growth for the different taken images (each colour) of the SN2023ixf data points for the sdssg band. Near 6 arcsec is the peak of the growth curve. The rise of S/N for higher apertures is due to the bulge of M101.

Both catalogues use the *SExtractor*[2] table structure, which includes numerous columns for different magni-

[2] https://sextractor.readthedocs.io/en/latest/index.html

tude definitions. For our analysis, we chose to extract light curves from the *MAG_APER* columns, which measure the magnitude of objects at various aperture sizes. We selected a ∼6 arcsec aperture for studying SN2023ixf because it corresponds to the highest signal-to-noise (S/N) ratio, as indicated by the growth curve shown in Figure 11.

With the peak of the growth curve identified, we can easily calculate the offset, which is the difference between the measured magnitudes at ∼6 arcsec in J-VAR and J-PLUS for the cross-matched reference stars in the M101 tile. Figure 12 illustrates the application of these offsets using one band as an example.

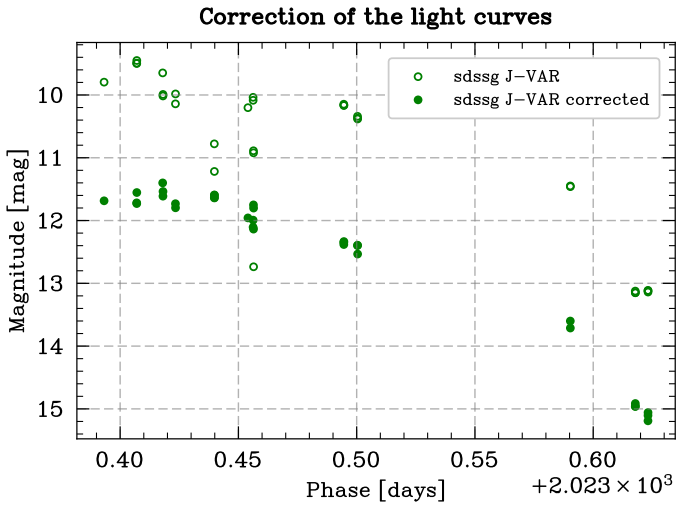

Figure 12: Light curve in gsdss band for SN2023ixf corrected by offsets (green filled circles) and not corrected by offsets (non-coloured circles). Thanks to the offset corrections, the dispersion of the light curves is fixed.

sncosmo model

Once the magnitudes were corrected using the calculated offsets and SN2023ixf was identified within the J-VAR field, we proceeded to analyze the light curve. In this case, we chose not to fit the light curve with a decay model (such as the Bazin function) due to significant issues that arose, leading to non-convergence of the model. This was likely caused by the limited number of data points and their wide temporal dispersion, a result of the J-VAR survey's methodology. Consequently, we opted to use the "nugent-sn2p" model instead.

The light curves extracted from J-VAR data for SN2023ixf across the different J-VAR filters (J0395, gsdss, J0515, rsdss, J0660, isdss, and J0861), corrected for offsets, are presented in Figure 13. Additionally, Figure 15 shows the fits for the 7 bands using "nugent-sn2p".

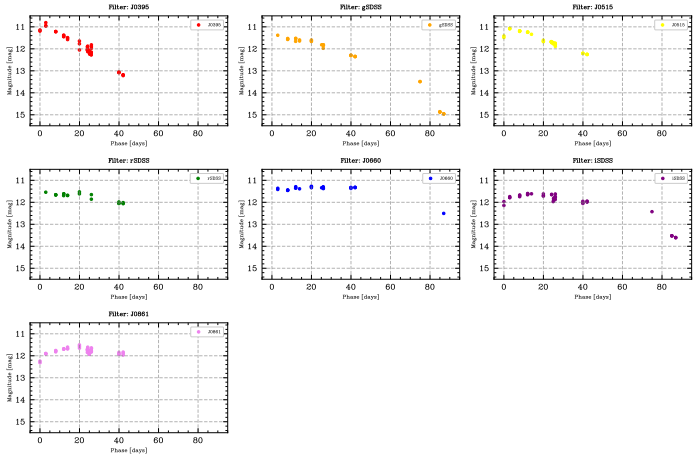

Figure 13: Light curves, using JAST80 data, for the SN2023ixf for all the J-VAR filters (J0395, gsdss, J0515, rsdss, J0660, isdss, and J0861), each one in a different panel. A plateau is noticeable in the reddest bands. The error bars are not noticeable because they are small.

Figures 13 and 15 reveal that the data points are quite temporally dispersed compared to the light curves obtained with the Tx40 telescope (Figure 8). Additionally, the "nugent-sn2p" model does not provide a robust fit, showing significant discrepancies in the reddest bands, as illustrated in Figure 15, resulting in a large reduced chi-squared value. Similar issues in the redder bands were also observed in the *sncosmo* fit for the Tx40 data (Figure 10), indicating that these *sncosmo* models may have inherent limitations in these bands.

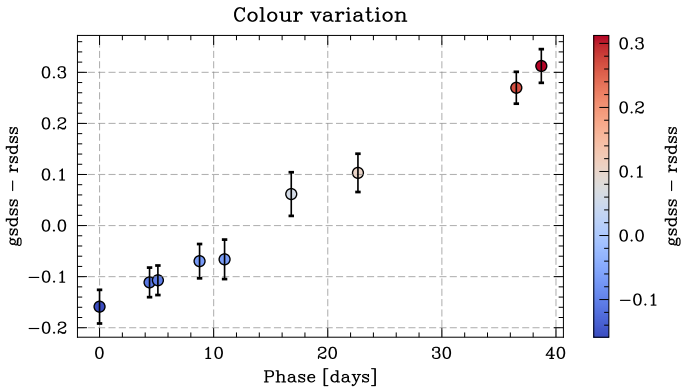

Figure 14: Colour (gsdss-rsdss) variation of SN2023ixf using JAST80 data. A redness with the phase is shown. The error bars are not noticeable because they are small.

Despite the issues encountered with the JAST80 data, the colour evolution of SN2023ixf can still be studied. Figure 14 shows the colour evolution (gsdss-rsdss) of SN2023ixf using JAST80 data. A reddening trend with time is observed, likely due to energy variations during the explosion and interactions with the interstellar medium (de Jaeger et al. 2018).

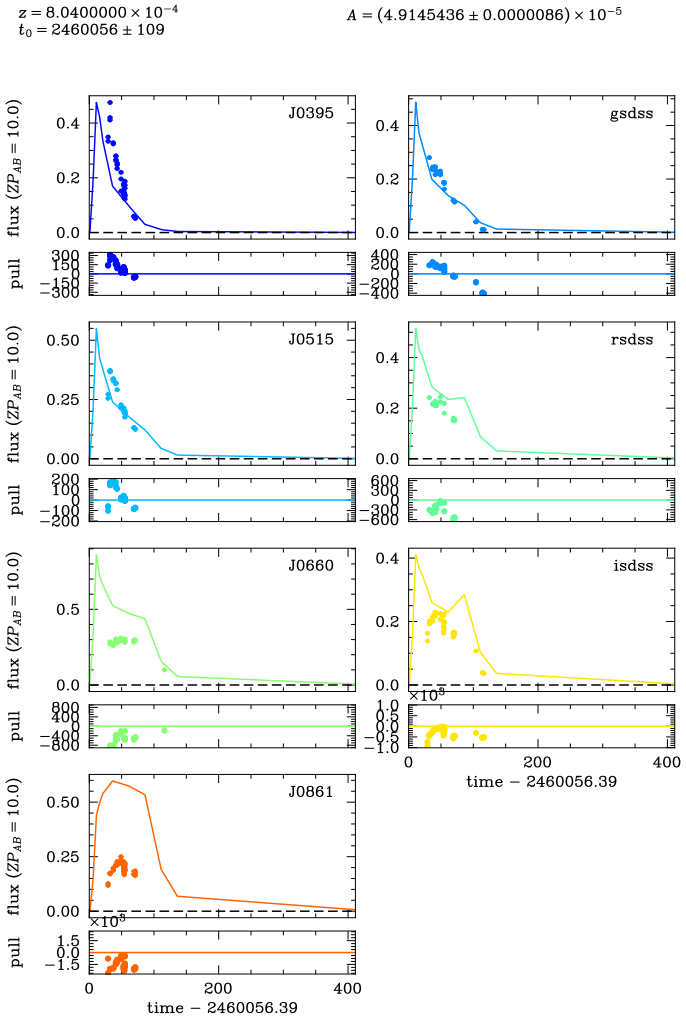

Figure 15: Light curves, using JAST80 data, fitted for the SN2023ixf by using the nugent-sn2p model for all the J-VAR filters (J0395, gsdss, J0515, rsdss, J0660, isdss, and J0861), each one in a different panel. Pulls correspond to errors associated with the differences between the observations and the model. The fitted model parameters A and t_0 are also fitted at the top. Huge discrepancies are shown in the reddest bands. The error bars are not noticeable because they are small.

While the data collected by the Tx40 telescope provided a solid foundation for studying SN2023ixf, the additional filters available from JAST80 offer more detailed information. However, we encountered significant challenges when fitting the light curves, particularly in the redder bands, using *sncosmo*, and faced issues with the non-convergence of the decay model. These difficulties likely stem from missing the peak of the light curve and the sparse, temporally dispersed data points, which are linked to the methodology of the *sncosmo* model. This last model should be studied in more detail to find future solutions for this part of the work. In addition, it is important to mention that the light curves of Tx40 and JAST80 have some discrepancies between them during the peak, which is something to keep in mind. (see Appendix C). Further details on SN2023ixf can be found in other studies, notably the work by Hiramatsu et al. (2023).

7 PESSTO

The second part of this study focuses on the PESSTO (Public ESO Spectroscopic Survey of Transient Objects) project. As detailed in Section 4, PESSTO utilizes the ESO's New Technology Telescope (NTT) equipped with both optical (EFOSC2) and near-infrared (SoFi) spectrographs to classify and monitor transient astronomical phenomena, such as supernovae and other unusual optical events. Figure 16 presents the distribution of various types of transients observed in PESSTO, with supernovae (SNe) comprising the majority. Notably, Type Ia supernovae (SNIa) are the most frequently observed transient type.

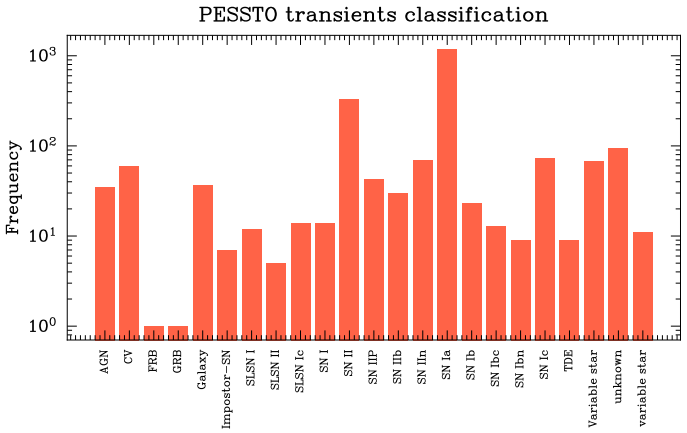

Figure 16: Logarithmic bar distribution of the different transients classification in PESSTO. SNe dominate the distribution, in particular, SNIa is the most common transient type.

PESSTO provides spectral measurements at different times for all observed transient objects, allowing us to study the evolution of emission lines in supernovae (SNe). While some SNe in the PESSTO catalogue have only one or two spectral observations, others have multiple spectra. The latter is the focus of this study, as more spectral data points enhance the light curve, increasing the likelihood of accurately fitting the curve. Consequently, transients with more spectral measurements are particularly valuable for detailed analysis. Figure 17 highlights the 20 PESSTO transients with the most extensive spectral coverage.

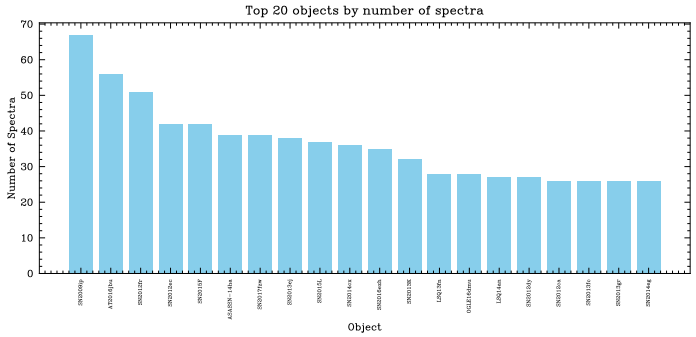

Figure 17: The 20 transients PESSTO objects with the most spectra measured. SNe dominates the bar distribution.

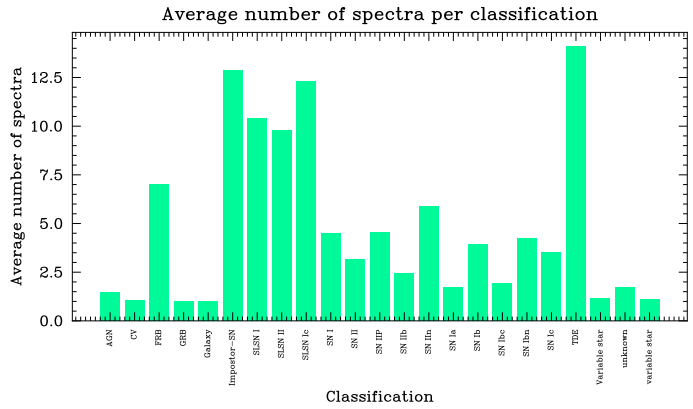

Figure 18: Average number of spectra per type of transients. It is important to note the few averages for the SNe, which is a problem for making our accurate study.

As mentioned earlier, we focus on studying SNe with multiple spectra. However, a significant challenge is that the majority of SNe in the PESSTO dataset have fewer than 5 spectral measurements. This limitation translates to fewer than 5 points on the light curve, which is insufficient for applying models like the Bazin function to accurately fit the curve. Consequently, despite PESSTO's extensive collection of SNe, only a small subset can be effectively utilized in this study. Figure 18 illustrates the average number of spectra per transient type, clearly showing the low average for SNe.

7.1 Spectra

Given the extensive spectral evolution data collected by the PESSTO survey for various objects, we can visualize this information in multiple ways to better understand transient behaviour. As an example, Figure 19 illustrates the spectral evolution of SN2013K, a Type IIP supernova.

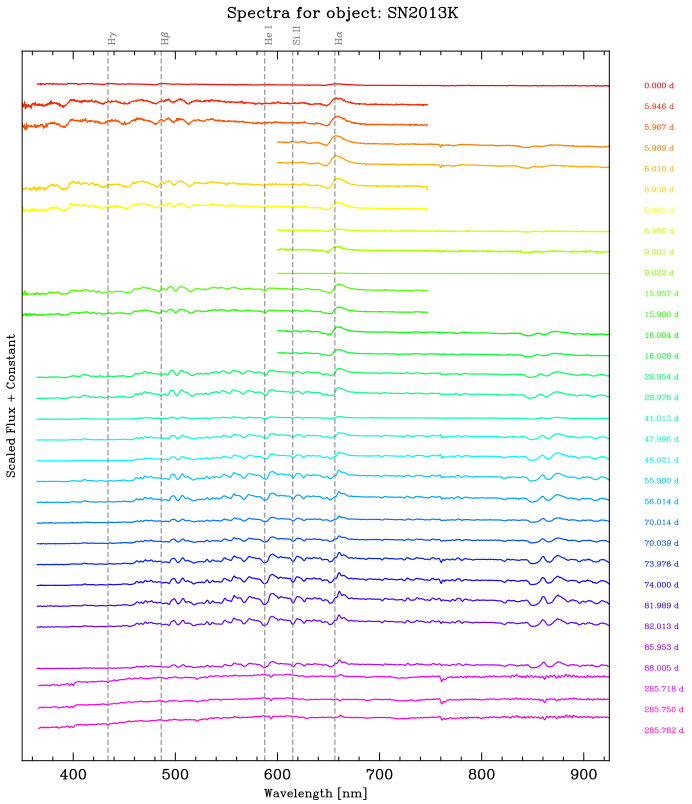

Figure 19: Spectra evolution of the SN2013K, a Type SN IIP. From top to bottom, the SED (Spectral Energy Distribution) is shown from the first measured to the last. Lines evolution is seen. Due to the different grisms used to take the measurements, different ranges of wavelength are covered. Dashed grey vertical lines show the positions of the typical lines (from left to right, Hγ, Hβ, HeI, SiII, and Hα) needed to classify an SN from each spectrum.

Another compelling way to visualize spectral evolution is by plotting the light curve in a three-dimensional

plane, where the wavelength is represented on the y-axis. Figure 20 illustrates this light curve plane for SN2015F, a Type Ia supernova.

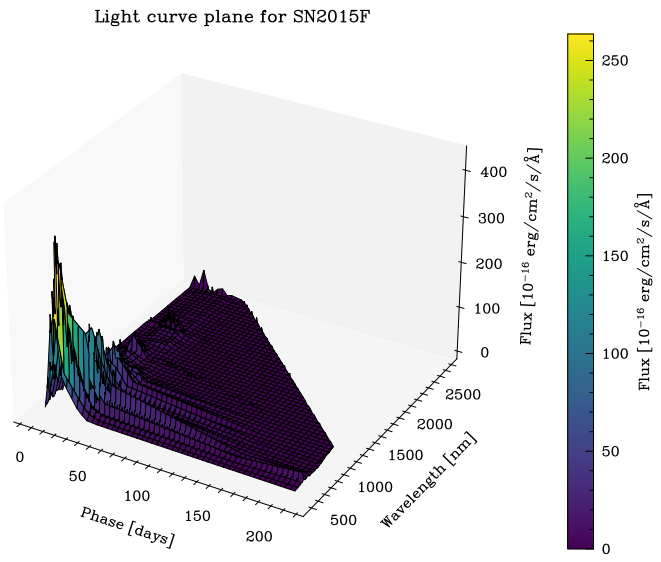

Figure 20: Light curve plane (phase vs wavelength vs flux) for SN2015F, a Type Ia supernova. Emission lines at the beginning of the phase show a non-variable spectrum. From the day of the 50th, new emissions lines started to change and rise in flux.

7.2 Light and colour curves

We have presented the light curve plane (Figure 20), which provides valuable insights. However, it is also crucial to determine whether we can derive light curves for the seven J-VAR filters using synthetic photometry. This is important because the goal of this work is to classify supernovae (SNe) using J-VAR, which requires a large SNe catalogue like PESSTO. Since PESSTO primarily collects spectra, synthetic photometry is necessary to analyze the light curves in the various J-VAR filters.

Utilizing the spectral data from PESSTO, we employed different tools to perform synthetic photometry and calculate the magnitudes for the seven J-VAR bands. For this purpose, we chose the *sncosmo* package in Python, which includes functions that allow us to derive magnitudes using the spectra and transmission curves of the J-VAR bands. By applying this method, we computed synthetic magnitudes for the seven bands across all transients classified in PESSTO. Figure 21 presents the light curves of some transients from the PESSTO catalogue.

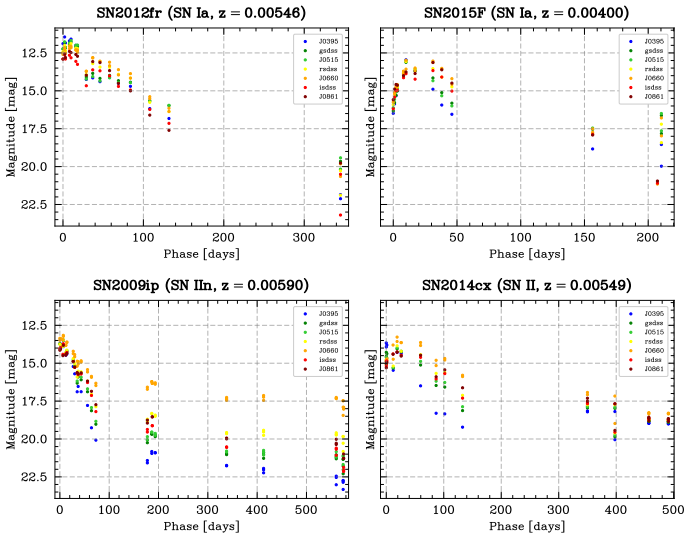

Figure 21: Light curves for some of the PESSTO's transients (in each panel) for all the J-VAR filters (J0395, gsdss, J0515, rsdss, J0660, isdss and J0861). Different shapes of light curves can be seen for the different types of transients. The name, type and redshift of the transient are shown in the title.

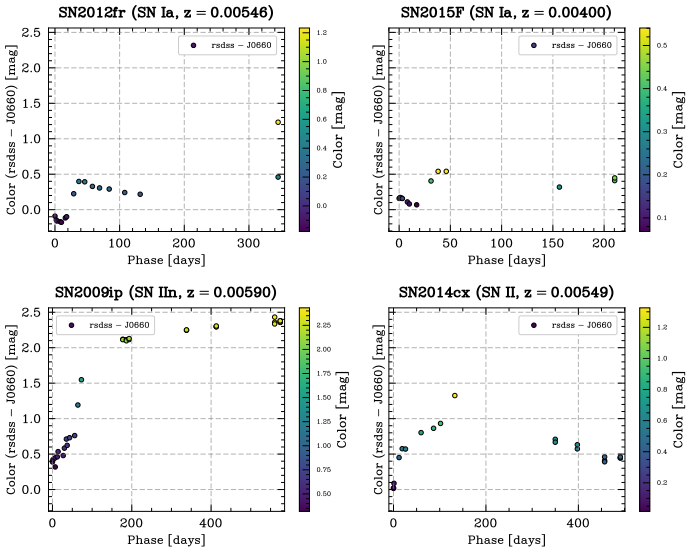

Figure 22: Colour (rsdss - J0660) curves for some of the PESSTO's transients (in each panel). Different shapes of colour curves can be seen for the different types of transients. The rsdss - J0660 colour variation has been chosen to notice the evolution of the Hα line and each association for SNe II. The name, type and redshift of the transient are shown in the title.

Additionally, we can study the colour variation of su-

pernovae. Figure 22 displays the colour curves for several transients classified in PESSTO. The rsdss—J0660 colour variation has been selected to highlight the evolution of the Hα line, which is notably associated with Type II supernovae.

As shown in Figure 22, Type II SNe exhibits significant colour variation, whereas Type Ia SNe do not. This distinction serves as an initial method for classifying and differentiating between these SN types. Another way to distinguish them is by observing the shape of their light curves (see Figure 21). While Type Ia SNe display a rapid decline in their light curves, Type II SNe exhibit a slower decline, either in the form of a plateau or a linear descent.

7.3 SN classification: stretch method

Throughout this report, we've discussed various methods for classifying supernovae. One significant approach is by analyzing the shape of their light curves. This method is particularly valuable as it provides extensive information about the progenitor type and the evolution across different photometric bands. However, a major drawback is that it requires continuous monitoring throughout the explosion period (approximately a month), with measurements needed both before and after the peak brightness.

In contrast, the spectroscopic method, which classifies SNe using only one or two spectra taken before, during, or after the peak, offers an alternative. This method, employed by PESSTO, doesn't yield detailed light curve information but instead provides insights into the evolution of emission lines. If sufficient spectra are available, synthetic photometry can be used to estimate the light curve, as demonstrated in Section 7.2. In this subsection, we explore another classification technique known as the stretch method.

The stretch method involves re-scaling the time-axis of light curves by applying a stretch factor s, where $t' = (1/s) \cdot t$. This transformation adjusts the light curve, making it appear narrower or wider. The core idea is to select reference light curves for each SN type and then apply the stretch factor to other light curves to match the shape of the reference. By iteratively applying the stretch factor, the goal is to transform the light curves so they resemble the reference curve, creating a template for each SN type. This template can then be used to classify new SNe by overlaying their light curves onto the template. Additionally, normalization of magnitudes is applied to ensure all light curves share the same peak magnitude, further aiding in the comparison process. Figure 23 provides a visual example of the stretch method.

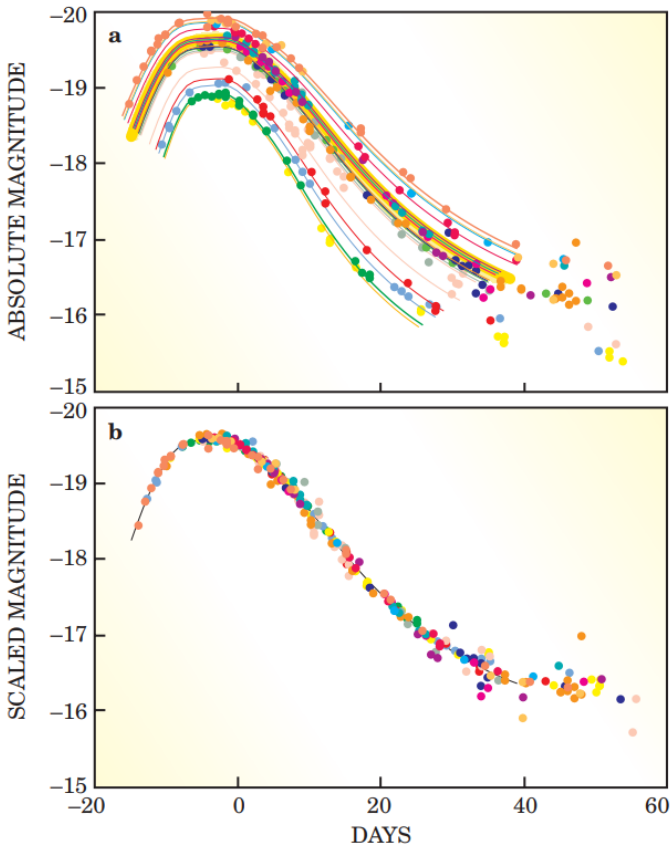

Figure 23: Curve lights of SNe before (top) and after (bottom) applying the stretch method. Figure extracted from Perlmutter (2003).

To apply the stretch method effectively, it's essential to fit the light curves accurately. In our research, we opted to use the spline fitting method rather than the Bazin functions or *sncosmo* models. This decision was primarily due to the limitations posed by the PESSTO dataset, where many SNe have only one spectrum, which provides just a single point on the light curve. This makes it impossible to perform reliable light curve fits using the other methods.

In some cases, we had more data points, but it's important to note that fitting light curves with the Bazin function requires at least five points. Similarly, using *sncosmo* for fitting can lead to significant issues when only a few points are available, especially on small scales.

Therefore, we chose the spline method for fitting the light curves. However, it's worth mentioning that some SNe were excluded from the analysis because the spline method did not accurately represent their typical behaviour. This is a known limitation of splines, as they can

sometimes introduce artefacts like a second peak, which is not characteristic of standard supernova light curves.

Figure 24 illustrates an example of the stretch method applied to a Type Ia SN, having the reference and the science light curve.

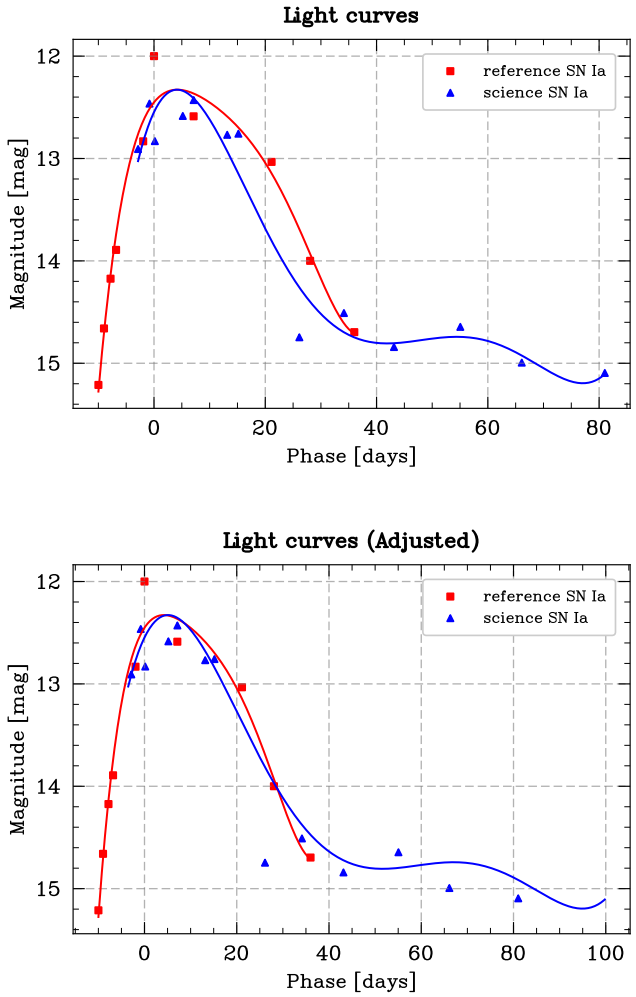

Figure 24: Curve light of an SN before (top) and after (bottom) applying the stretch method. In the red solid line, the spline fit for the reference reference SN light curve. In a blue solid line, the spine fit for the science (the one for which the stretch method is applied) SN light curve. It is shown how the stretch method changes the shape of the science light curve thus resembling the reference one. The SN Ia type was chosen for this example.

Once the stretch method was understood and successfully implemented for a single case, the next step was to apply it to all the SNe in the PESSTO dataset, focusing specifically on the J-VAR filters. The first objective was to apply the stretch method to Type Ia SNe using the sdssg (green) filter. Figure 25 presents the results of this application, showing the stretched and normalized light curves for all Type Ia SNe in PESSTO.

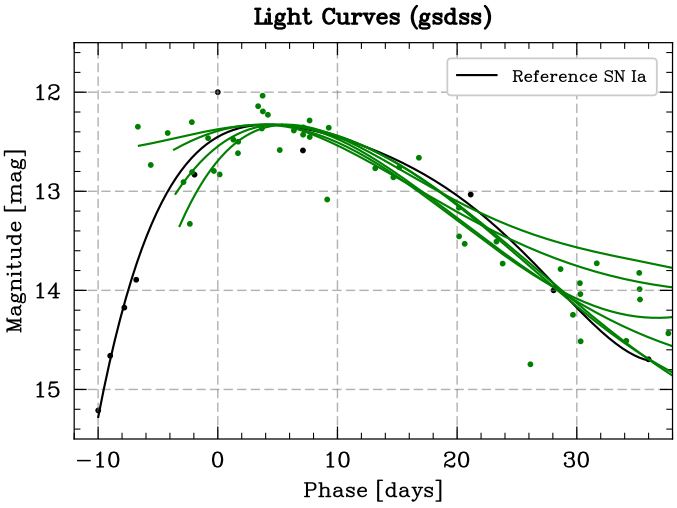

Figure 25: Stretch method applied for the SNe Ia from PESSTO for the gsdss filter. Few SNe are only shown because of the selection criteria (more than 5 spectra a 0.7 $< s <$ 1.3). Green dots correspond to the green light curves while the black dots to the reference Type Ia SN light curve.

It is important to note that PESSTO contains data for over 1.000 Type Ia SNe, but only 8 are shown in Figure 25. This limitation arises because, as previously mentioned, most SNe in the dataset have fewer than 5 spectra, making it difficult to study their light curves in detail. Additionally, we selected only those SNe with a stretch factor between 0.7 and 1.3, as these displayed typical behaviours (a single peak without significant displacement).

Following this, we extrapolated the results to the other bands for Type Ia SNe. Figure 26 illustrates the application of the stretch method across all J-VAR filters using Type Ia SNe from PESSTO.

As observed in Figure 26, the stretch method did not yield consistent results across all bands. While the rsdss band produced relatively acceptable outcomes, the results for the other bands were chaotic, with the Hα filter (J0680) being the most problematic. These findings suggest that for the stretch factor to be effectively applied across all 7 J-VAR bands, a more extensive catalogue of SNe is necessary. This catalogue should contain more data points both before and after the peak, with measurements taken at regular intervals. Additionally, using

actual photometric data instead of synthetic photometry would likely improve the results. In addition, we have tried other types of model fits (e.g.: interpolation), but the same problems were found. In conclusion, future works and observation will enable us to make templates for the different types of SNs for the 7 J-VAR filters, which was the main aim of this work.

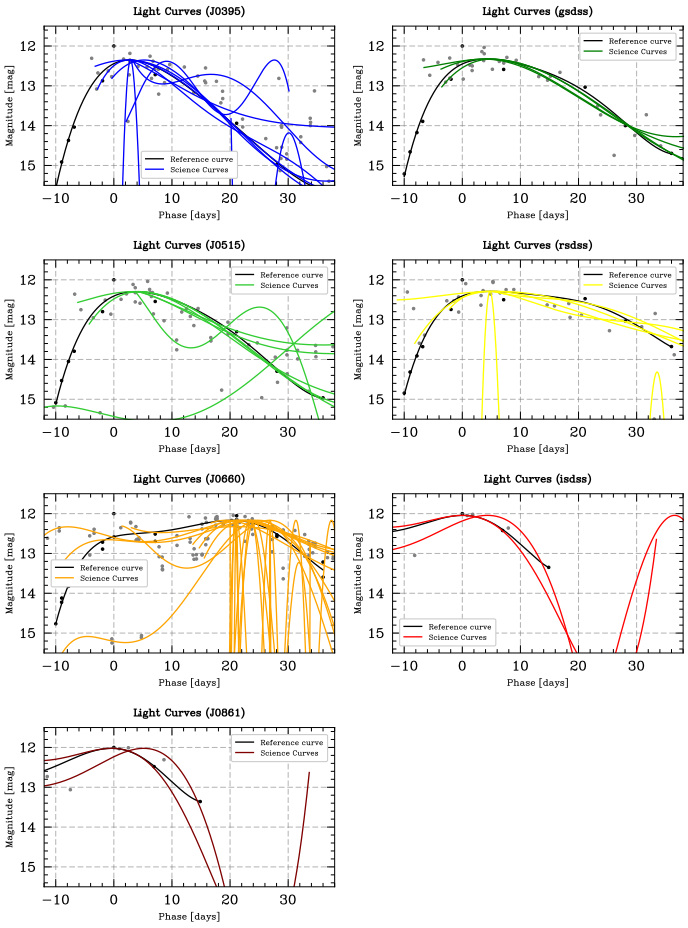

Figure 26: Stretch method applied for the SNe Ia from PESSTO for all the J-VAR filters. Few SNe are only shown because of the selection criteria (more than 5 spectra a $0.7 < s < 1.3$).

The same study was done on Type II SNe. The results have the same problem and are shown in Appendix B

Finally, Appendix Appendix A has a URL to GitHub that collects all the code, in jupyter notebooks, used for doing this report, in case you are interested in the calculation process.

8 Conclusion

The initial analysis of the supernova SN2023ixf, discovered in the M101 galaxy, has provided valuable insights into its light curve and subsequent classification. The data gathered from the Tx40 telescope, despite starting observations post-peak, has offered a significant foundation for understanding the supernova's light curve (Figure 8). The application of the Bazin decay model facilitated the characterization of the light curves across different sdss bands, yielding parameters that align closely with established standards, albeit with notable deviations in the τ_{rise} parameter (Table 1 and 2). This discrepancy underscores the challenges posed by the absence of pre-peak data, which may have skewed the estimation of the rise time.

The analysis further demonstrates that SN2023ixf conforms to the characteristics of a Type IIP supernova, evidenced by its light curve's plateau phase and a relatively short τ_{fall} all. This classification was corroborated through fitting with the "nungent-sn2p" model from the *sncosmo* package, though some discrepancies, particularly in the redder bands, highlighted potential limitations of the model (Figure 10). The observed secondary peak predicted by the sncosmo model in the redder bands, inconsistent with the known properties of Type IIP supernovae, suggests the need for further model refinement or the exploration of alternative fitting approaches.

The additional data from the JAST80 telescope, despite its advantages in covering multiple filters, presented its challenges. The variability in data quality, due to less favourable observational conditions and a sparse dataset, complicated the light curve fitting process. Since we were unable to converge the fit using the Bazin function, we opted for the synchronization models. However, the difficulties encountered with the *sncosmo* model, particularly with its non-convergence and the substantial discrepancies in the redder bands, point to inherent limitations that warrant further investigation (Figure 15). The observed colour evolution (Figure 14) of SN2023ixf, as revealed by JAST80 data, indicates a reddening trend that aligns with theoretical expectations related to supernova energy variations and interactions with the interstellar medium.

The PESSTO (Public ESO Spectroscopic Survey of Transient Objects) project represents a significant advancement in the field of transient astronomical phenomena, leveraging the capabilities of the ESO's New Technology Telescope to provide a rich dataset of spectral observations. As detailed in the preceding sections, the PESSTO

survey has amassed a comprehensive collection of spectra for various transient events, with a particular emphasis on supernovae (SNe). This extensive dataset allows for detailed analyses of transient objects, particularly through the evolution of emission lines and light curves. However, the study also highlights both the strengths and limitations inherent in the PESSTO dataset.

The most prominent finding from our analysis is the overwhelming dominance of Type Ia supernovae (SNIa) within the PESSTO dataset (Figure 16). These SNe are observed more frequently compared to other transient types, which has facilitated a deeper understanding of their light curve characteristics and spectral evolution. The availability of multiple spectra for certain SNe enhances the quality of the light curve fits, making these objects particularly valuable for detailed studies. Figures illustrating spectral evolution and light curves underscore the potential of this data to shed light on the temporal changes in supernovae and other transient objects.

One of the primary challenges identified in this study is the limited number of spectral measurements available for most SNe (Figure 18). The dataset reveals that a significant proportion of SNe in PESSTO have fewer than five spectral observations (Figures 19 and 20). This limitation impacts the ability to apply sophisticated models, such as the Bazin function, for accurately fitting light curves. Consequently, despite the wealth of data, only a subset of SNe with extensive spectral coverage can be effectively utilized for detailed analysis. This constraint emphasizes the need for more frequent and comprehensive spectral monitoring to improve the robustness of light curve fits and subsequent analyses.

Our exploration of synthetic photometry to derive light curves for J-VAR filters highlights the potential and limitations of this approach. While synthetic photometry enabled the calculation of magnitudes across different bands, the results varied significantly. The challenges observed, particularly in the Hα filter and other bands, suggest that future improvements in observational strategies are necessary. A more extensive catalogue with frequent measurements, as well as the use of actual photometric data rather than synthetic methods, would likely enhance the accuracy and reliability of light curve analyses.

The stretch method (Figures 23 and 24) applied for supernova classification reveals both its potential and limitations. While the stretch method offers a valuable technique for classifying SNe based on the shape of their light curves, the effectiveness of this approach was inconsistent across different J-VAR filters. The results demonstrated that while some bands, like the sdssg filter, provided acceptable outcomes, others exhibited chaotic results (Figure 26). This inconsistency underscores the need for more robust datasets with greater coverage to ensure accurate classification across all filters.

In conclusion, the study of supernova SN2023ixf and the PESSTO dataset highlights both advancements and challenges in our understanding of transient astronomical phenomena. Despite the initial success in characterizing SN2023ixf as a Type IIP supernova and the valuable insights provided by the Tx40 and JAST80 telescopes, the limitations imposed by incomplete pre-peak data and variable observational conditions underscore the need for further refinement in modelling techniques and observational strategies. The PESSTO project, with its extensive collection of spectra, offers a robust foundation for analyzing supernovae, particularly Type Ia, but also reveals significant gaps in spectral coverage that impact the accuracy of light curve fitting and classification. Future research would benefit from more frequent and comprehensive spectral monitoring, along with improvements in synthetic photometry and data analysis methods, to enhance our understanding of supernovae and transient events. Continued efforts to address these challenges will be crucial for advancing the field and refining our models and classifications of these fascinating celestial phenomena.

Appendix A: Code

For the execution of this project, we have developed several Jupyter notebooks covering different aspects of the work. You can find all the code, data, referenced papers, and key figures collected in these notebooks at the following GitHub repository: https://github.com/juananmol/Internship_CEFCA.git

Appendix B: Templates for Type II SNe

In Subsection 7.3, we attempted to create templates for Type Ia supernovae using the stretch method. The goal was to develop templates for the 7 J-VAR filters to facilitate a classification algorithm based on light curves detected with OAJ. However, we encountered significant issues, and the templates could not be successfully constructed. We then applied the same approach to Type II supernovae, but unfortunately, we faced similar difficulties, resulting in chaotic templates for this type of supernova as well. Figure 27 illustrates the results obtained.

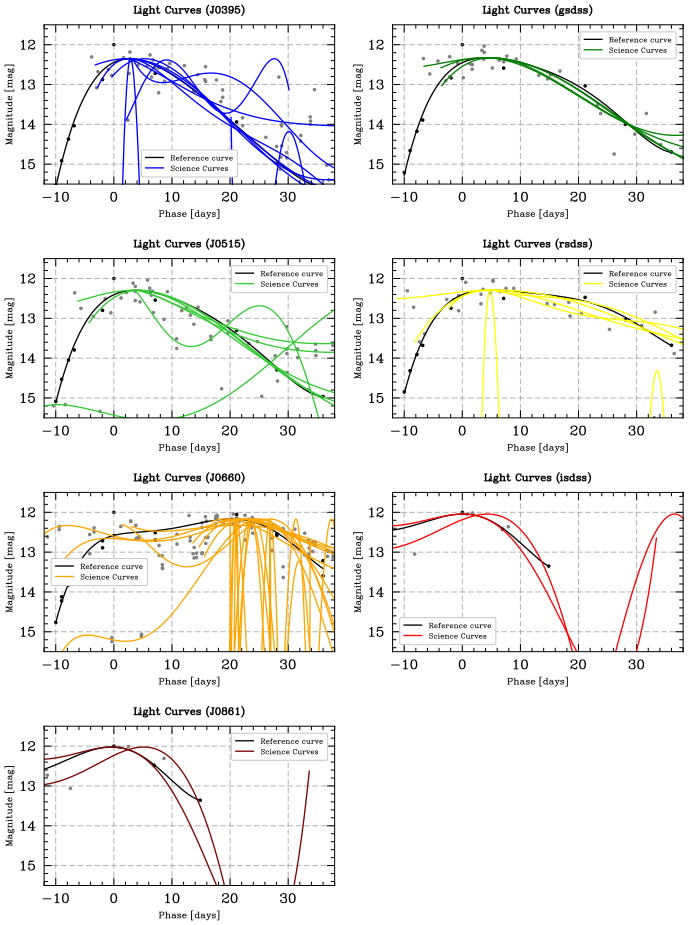

Figure 27: Stretch method applied for the SNe II from PESSTO for all the J-VAR filters. Few SNe are only shown because of the selection criteria (more than 5 spectra a $0.7 < s < 1.3$)

Appendix C: Correlation between Tx40 and JAST80 light curves

The supernova SN 2023ixf has been observed using two telescopes from OAJ: Tx40 and JAST80. Both telescopes provided light curves for this SN; however, when the curves were compared, some discrepancies were observed during the peak. Figure 28 shows the discrepancies for the gsdss bands. However, the same problems are present in the rsdss and isdss bands.

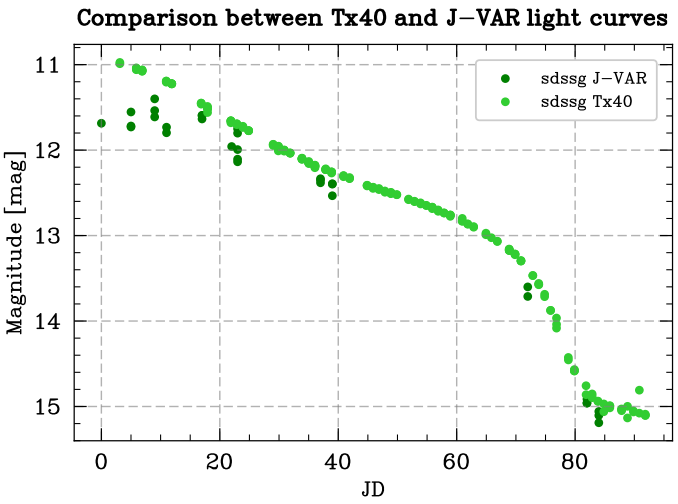

Figure 28: Light curve of SN 2023ixf using Tx40 (light green dots) and JAST80 (dark green dots) data. Some discrepancies during the peak are found.

References

Bazin, G., Palanque-Delabrouille, N., Rich, J., et al. 2009, aap, 499, 653

Dai, M., Kuhlmann, S., Wang, Y., & Kovacs, E. 2018, mnras, 477, 4142

de Jaeger, T., Anderson, J. P., Galbany, L., et al. 2018, mnras, 476, 4592

Hiramatsu, D., Tsuna, D., Berger, E., et al. 2023, apjl, 955, L8

Perlmutter, S. 2003, Physics Today, 56, 53

Pledger, J. L. & Shara, M. M. 2023, apjl, 953, L14

Rau, A., Kulkarni, S. R., Law, N. M., et al. 2009, pasp, 121, 1334

Turatto, M. 2003, in Supernovae and Gamma-Ray Bursters, ed. K. Weiler (Berlin: Springer), 21–36